energies

MDPI

Article

Construction of Transmission Line Segments Assessment Model Based on Correlation Analysis and Analytic Hierarchy Process Method

Shizeng Liu [1], Yigang Ma [1], Wenbin Yu [1], Xianzhong E [1], Yang Huang [2], Jiahao Liu [2] and Hongwei Mei [2,*]

[1] Dali Bureau, EHV Power Transmission Company of CSG, Dali 671014, China; 18987227073@163.com (S.L.); 15877739677@163.com (Y.M.); 15368729334@163.com (W.Y.); 18887201898@163.com (X.E.)
[2] Shenzhen International Graduate School, Tsinghua University, Shenzhen 518055, China; huang-y22@mails.tsinghua.edu.cn (Y.H.); 15889459695@163.com (J.L.)
* Correspondence: mei.hongwei@sz.tsinghua.edu.cn

Abstract

The reliable operation of transmission lines is essential for grid stability. Growing electricity demand pushes existing lines to full capacity, while new construction is constrained by resources and the environment. Dynamic capacity increase technology addresses this by boosting transmission capacity without physical upgrades, with the identification of weak points along the line being central to its application. This study integrates correlation analysis and the Analytic Hierarchy Process to develop an evaluation method for transmission line segments, with a supporting software implementation also developed. A system of characteristic quantities was first established using operation and maintenance guidelines combined with correlation analysis. The Analytic Hierarchy Process was applied to score features and derive weights after consistency validation. Preprocessed line data were then weighted to calculate segment weakness levels, and fuzzy comprehensive evaluation was used for both qualitative and quantitative condition analysis. The model was validated through a case study, and its software implementation streamlines and enhances the assessment process.

Keywords: line segments; dynamic capacity increase; correlation analysis; analytic hierarchy process; evaluation software

1. Introduction

Electricity supply and security are essential components of national security strategies and significantly impacting economic and social development. In recent years, driven by rapid economic growth, there has been a sharp increase in the demand for electricity across society [1–3]. Concurrently, the integration of renewable energy sources such as wind power and photovoltaic power has put significant strain on the transmission capacity of the system. Transmission lines, as fundamental elements of the grid, often operate at heavy loads or even full capacity on a daily basis. This inability to keep pace with the continuous growth in demand severely affects the power supply capacity of the grid [4–6]. For instance, in Punjab, India, the peak power demand has nearly doubled over the past decade, from approximately 9074 MW in 2012–2013 to 17,233 MW in 2025. This growing demand has caused the grid to operate at or near its maximum capacity, necessitating significant expansions in both generation and transmission capabilities to ensure a reliable supply. To meet the demand for electricity, especially to reduce operational risks under the

Check for updates

Academic Editor: Anastasios Dounis

Received: 31 January 2026
Revised: 26 February 2026
Accepted: 5 March 2026
Published: 9 March 2026

Copyright: © 2026 by the authors. Licensee MDPI, Basel, Switzerland. This article is an open access article distributed under the terms and conditions of the Creative Commons Attribution (CC BY) license.

N−1 operating mode (which means that the grid must withstand the loss of any single critical element—line, transformer, or generator—and continue operating securely without cascading failures), a large number of transmission lines need to be either constructed or reconstructed. However, this endeavor faces substantial challenges, including significant manpower and material resource demands, lengthy construction periods, and constraints such as difficulties in acquiring transmission line segments for construction and environmental protection issues [7,8]. Therefore, achieving an increase in transmission capacity without altering the distribution of existing transmission corridors is of great significance for ensuring the safe, economic, and reliable operation of the power grid, which is the core objective of dynamic capacity increase technology for transmission lines [9]. Existing studies have shown that considering the dynamic capacity increase effect in the design and operation of transmission lines, combined with the analysis of historical meteorological information, can further tap into the potential transmission capacity of the lines and enhance the economic efficiency of system operation [10].

The dynamic capacity increase technology of transmission lines faces various challenges, such as the assessment of transmission line segments and how to maximize measurement redundancy when the number of Phasor Measurement Unit (PMU) channels is limited [11–13]. Among these, transmission line segment assessment is a key component and is also the research focus of this paper. The purpose of transmission line segment assessment is to identify weak points in the line to ensure its safe and stable operation during the capacity increase process and to prevent accident risks [5].

Currently, traditional methods for assessing transmission line segments primarily rely on operational guidelines or expert judgment [14–16]. Although these methods are straightforward and practical, they have certain limitations. Operational guidelines are usually uniformly formulated within the power grid, making them less adaptable to different regions and environments [17,18]. Furthermore, expert judgment is susceptible to subjective biases, lacking objectivity and scientific rigor, thereby limiting the accuracy of assessment results. Therefore, there is an urgent need to develop a scientifically sound and objective transmission line segment assessment model to improve the accuracy and reliability of assessment results and ensure the safe operation of transmission lines.

To address these challenges, this paper proposes a transmission-line segment assessment framework that combines correlation analysis, AHP-based weighting, and fuzzy comprehensive evaluation [19,20]. Specifically, correlation analysis is first adopted as a data-driven screening step to examine the relationships among candidate characteristic quantities and to identify the most influential factors, thereby reducing subjectivity and ensuring that only statistically relevant variables are retained for subsequent evaluation. Next, the Analytic Hierarchy Process (AHP) is employed to determine the relative importance of the selected indices, because dynamic line rating (DLR)–related assessment involves both quantitative measurements and qualitative expert knowledge; AHP provides a systematic way to translate expert judgments into consistent numerical weights through hierarchical structuring. Furthermore, a fuzzy comprehensive evaluation is introduced to cope with the inherent uncertainty and vagueness in transmission-line operating conditions, where crisp binary classifications are often inadequate; fuzzy logic enables graded membership to better represent the continuous nature of line states.

Compared with purely machine-learning-based approaches that typically require large, labeled datasets, or purely deterministic models that may fail to capture uncertainty, the proposed hybrid framework is more suitable for the small-sample, multi-criteria decision-making setting commonly encountered in transmission-line segment assessment. Subsequently, the framework is validated using data from a local power grid to demonstrate its accuracy and effectiveness, and the software implementation of the proposed

assessment model is developed. The findings not only enable a more scientific and accurate assessment of transmission-line segments but also contribute to the advancement of dynamic capacity-increase technologies for transmission lines [21,22].

This paper is organized as follows. Section 2 introduces the construction process of the characteristic quantity system for assessing transmission line segments. Section 3 describes the principles and methods of the assessment process. Section 4 presents the analysis of arithmetic examples verify the accuracy and effectiveness of the model. Lastly, Section 5 concludes this paper.

2. Construction of the Characteristic Quantity System

The selection of appropriate features is crucial for efficiently and accurately assessing the condition of transmission line segments. Next, we introduce the methods used to obtain information on transmission line segments and the process of screening and constructing the relevant features [23].

2.1. Obtaining Transmission Line Information

The grid intends to extend dynamic capacity increase technology to most transmission lines, so the transmission line segment information we selected needs to have the characteristics of easy accessibility, versatility, and generalization, in order to avoid hindering the promotion of this technology due to a lack of characteristic quantities.

Through the cooperative operation of the grid's standing unmanned aircraft system and software platform, we can obtain transmission line segments information including the length of the segments, line arc sag, maximum temperature arc sag, arc sag distance to the ground, headroom hazardous points, cross-crossing situation, cross-burden elevation difference, callout elevation difference, tower height, tower top elevation, tower base elevation, angle coefficient, corner type and other parameters. The schematic diagram of the transmission line point cloud is shown in Figures 1 and 2. Due to the strong correlation between the carrying capacity of the transmission line and the meteorological conditions, and after communicating with the on-site operation and maintenance personnel about the safety of the power grid operation [24], we preliminarily selected five parameters related to the dynamic capacity increase technology of transmission lines: the length of the segments, line arc sag, maximum temperature arc sag, the status of headroom hazardous points, and the cross-crossing status.

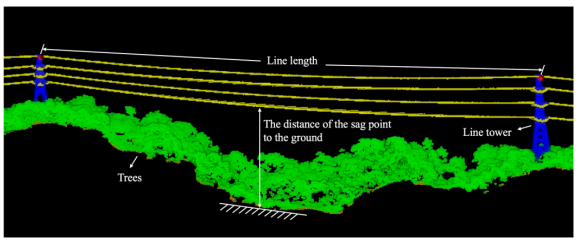


Figure 1. Point cloud map of transmission line generated by UAV 1.

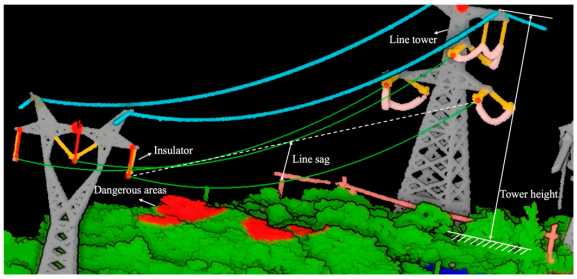


Figure 2. Point cloud map of transmission line generated by UAV 2.

2.2. Correlation Analysis to Extract Feature Quantities

First of all, we use data from a local power grid to carry out correlation analysis on the five preliminarily selected feature quantities. Correlation analysis can be performed by calculating the Pearson, Spearman, or Kendall correlation coefficient. Because there are few outliers in the data, we choose the Pearson correlation coefficient [25–27]. The Pearson correlation coefficient has the advantages of a clear value range, sensitivity to linear relationships, and low computational complexity, which makes it suitable for analyzing the linear relationship between variables.

The Pearson correlation coefficient, also known as the Pearson correlation index, is a statistical indicator that measures the strength and direction of the linear relationship between two variables. Its value ranges from -1 to 1, where 1 indicates a perfect positive correlation, -1 indicates a perfect negative correlation, and 0 indicates no linear correlation. The process of calculating the Pearson correlation consists of the following steps:

First, for two variables X and Y, calculate their means separately, as shown in Equation (1); then, calculate the covariance of X and Y, which indicates the degree of joint variation between the variables, as shown in Equation (2); then, calculate the standard deviation of X and Y, which indicates the degree of dispersion of the variables, as shown in Equation (3); and finally, using the results of the calculation of the covariance and standard deviation, calculate the Pearson correlation, as shown in Equation (4). The correlation visualization of the calculated Pearson coefficients is shown in Figure 3.

$$\overline{x} = \frac{1}{n}\sum_{i=1}^{n} x_i, \overline{y} = \frac{1}{n}\sum_{i=1}^{n} y_i \tag{1}$$

$$\mathrm{cov}(X, Y) = \frac{1}{n}\sum_{i=1}^{n} (x_i - \overline{x})(y_i - \overline{y}) \tag{2}$$

$$\sigma_x = \sqrt{\frac{1}{n}\sum_{i=1}^{n}(x_i - \overline{x})^2} \text{ and } \sigma_y = \sqrt{\frac{1}{n}\sum_{i=1}^{n}(y_i - \overline{y})^2} \tag{3}$$

$$\rho(X, Y) = \frac{cov(X, Y)}{\sigma_x \sigma_y} \tag{4}$$

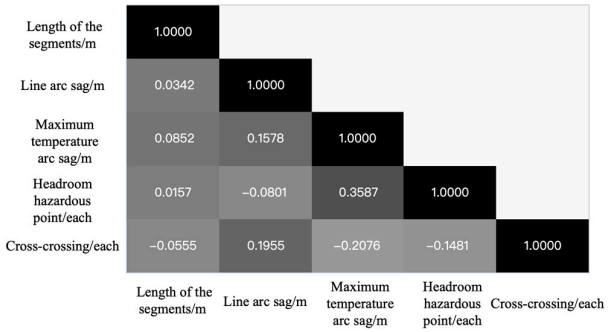


Figure 3. The initial Pearson correlation visualization.

The specific analysis shows that the correlation coefficients among segment length, sag, and maximum temperature sag are all greater than 0.9. As shown in Figure 3, the Pearson correlation coefficient between sag and maximum temperature sag reaches 0.98, indicating a high degree of linear correlation. This quantitative result clearly indicates the presence of information overlap between these two variables. At the same time, the clearance hazard point and cross-crossing items do not show significance with other parameters, and their correlation coefficients are close to 0, which means that these two features have high independence.

Since the Pearson correlation coefficient between arc sag and maximum temperature arc sag is close to 1, the two have a very strong positive correlation. In order to avoid the introduction of redundant information and to improve the stability of the model, the arc sag feature is discarded in the construction of the feature quantity system. Meanwhile, in order to consider the physical characteristics of the line more comprehensively, we take the ratio of the maximum temperature arc sag to the line length as a new feature quantity.

This quantity can more accurately reflect the influence of temperature and line length on the overall line condition, instead of only considering the absolute values of maximum temperature sag and line length, which improves the characterization ability of the model.

In addition, after comprehensively considering the key factors affecting the line in the dynamic capacity enhancement technology, two feature quantities, the channel environmental conditions and the number of historical clearances, are introduced. The channel environmental conditions, which mainly includes ventilation and lighting conditions, are factors that cannot be ignored when considering the thermal environment of the line. Ventilation conditions directly affect the flow of surrounding air, thus affecting the convection heat dissipation of the line, while lighting conditions are directly related to the radiant heat of the line. The introduction of the number of historical clearances as a characteristic quantity is based on its ability to reflect the tree barriers encountered by the line in the past operation, and it also provides an indicator of the stability and reliability of the line. In summary, the transmission line segments assessment feature quantity system is obtained as shown in Figure 4.

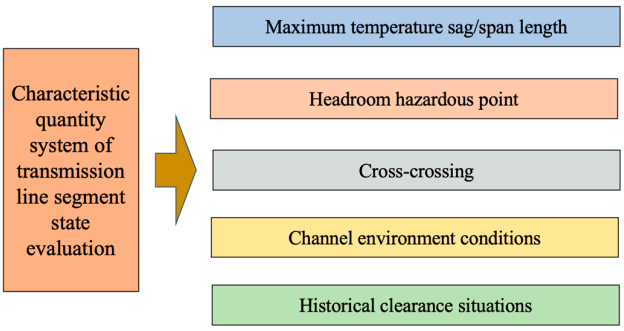


Figure 4. The evaluation feature system for the segment of transmission lines.

The results of the Pearson correlation analysis for these five features are shown in Figure 5. It can be clearly observed from Figure 5 that the absolute values of the correlation coefficients between all feature pairs are less than 0.1, and all p-values are greater than 0.05. This statistical result quantitatively demonstrates that the five characteristics—maximum temperature sag/segment length, headroom hazardous points, cross-crossing situations, channel environmental conditions, and historical clearance situations—are independent of each other, satisfying the requirement for feature independence in subsequent modeling.

It should be noted that the data used in this study were obtained from the internal transmission line operation data provided by China Southern Power Grid. In accordance with the company's data management regulations, these data involve the information security of power grid operation and cannot be disclosed publicly. Figures 3–5, and the related charts are all based on the aforementioned internal data, with data processing and visualization performed using MATLAB R2021b software.

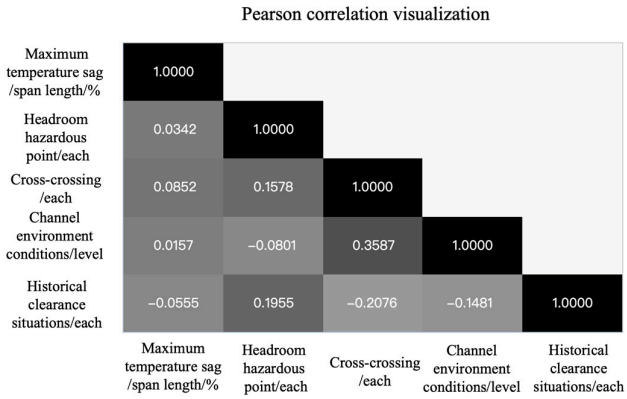


Figure 5. The final feature system Pearson correlation visualization.

3. Transmission Line Segments Assessment Computational Model

3.1. Weight Allocation Based on Analytic Hierarchy Process

The hierarchical analysis method (AHP) is an organic combination of quantitative and qualitative analysis, utilizing the actual experience of the decision makers to determine the degree of importance between the evaluation objectives.

By doing so, the relative weights of the characteristic quantities can be reasonably determined and effectively applied to problems that are difficult to solve by quantitative analysis. In order to enable quantitative operation, researchers have introduced the method of 9-ratio scaling, using aij to indicate the importance of factor i relative to j. The rules are shown in Table 1.

Table 1. Scale meaning of judgment matrix.

Scale	Definition
1	Two indicators are equally important
3	Importance of the former relative to the latter: slight
5	Importance of the former relative to the latter: a little
7	Importance of the former relative to the latter: strong
9	Importance of the former relative to the latter: extremely
2, 4, 6, 8	Denotes the middle value of the importance of above scales
reciprocal	Indicates the importance of the latter relative to the former

(1) Establish the hierarchical structure model: On the basis of in-depth analysis of the problem, the decision-making goals, decision-making objects and other relevant factors are stratified, because this model is only for the assessment of the weakness of the transmission line segments, so it only needs to be divided into the target layer and the feature quantity layer.

(2) Construct the judgment matrix: According to the five characteristic quantity indices, several field personnel with operation and maintenance experience were invited to score them pairwise according to the nine-ratio scale method. After taking the average value, the judgment matrix of the hierarchical analysis method is shown in Table 2 (the five feature quantities are recorded as k_1 to k_5 according to the order of maximum temperature sag/span length, headroom hazard point, cross-crossing situation, channel environmental situation and historical clearance situation).

In the table, A is the judgment matrix of the assessment index system, a_{ij} is the corresponding element in it, and $\mathbf{k_1}$–$\mathbf{k_5}$ denote the five feature quantities, respectively.

Table 2. Analytic hierarchy process judgment matrix.

A	k_1	k_2	k_3	k_4	k_5
k_1	1	4	2	1/2	1
k_2	1/4	1	1/2	1/9	1/4
k_3	1/2	2	1	1/4	1/2
k_4	2	9	4	1	2
k_5	1	4	2	1/2	1

(3) Consistency test. When constructing the judgment matrix, logical problems may be encountered. For example, there may be cases where a is more important than b, and b is more important than c, but c is considered more important than a. Although the probability of this situation is small, it is still necessary to carry out a consistency test to verify the reasonableness of the judgment. The formulas for the consistency test are shown in Equations (5) and (6).

$$\mathrm{CI} = \frac{\lambda_{max} - n}{n - 1} \tag{5}$$

$$\mathrm{CR} = \frac{CI}{RI} \tag{6}$$

where n is the order of the judgment matrix; λ_{max} is the largest eigenvalue; CI is the consistency index; CR is the consistency ratio; RI is the average random consistency index, and the corresponding consistency index value of each order matrix is shown in Table 3. The larger the value of CI is, the worse the consistency of the judgment matrix. When CR < 0.1, the judgment matrix can be considered to have satisfactory consistency.

Table 3. The corresponding consistency index value.

n	1	2	3	4	5	6	7
RI	0	0	0.52	0.89	1.12	1.24	1.36

Using MATLAB to write a relevant program can yield a consistency index (CI) of 0.00041639 and a consistency ratio (CR) of 0.00037178. Since CR < 0.1, this requirement is met, suggesting that the judgment matrix obtained above is consistent.

(4) Obtaining weights. There are usually three methods for obtaining weights: the arithmetic average method, the geometric average method and the eigenvalue method. The specific calculation of each method is as follows:

(a) Arithmetic average method. First, the judgment matrix is normalized by column; i.e., each element is divided by the sum of the column in which it is located. Then, the rows of the normalized matrix are summed. Finally, the weight vector is obtained by dividing each element of the resulting vector by the number of features. The formula for calculating the weight vector is shown in Equation (7).

$$\omega_i = \frac{1}{n} \sum_{j=1}^{n} \frac{a_{ij}}{\sum_{k=1}^{n} a_{kj}} \tag{7}$$

where i = 1, 2, . . ., n; n is the number of feature quantities.

(b) Geometric averaging method. $\boldsymbol{A}$ new set of column vectors is obtained by row multiplying the elements in each row of matrix $\boldsymbol{A}$. Next, the weight vector is obtained by performing the nth -root operation on each element of these new values followed by normalization. The formula for the weight vector is shown in Equation (8).

$$\omega_i = \frac{\left(\prod_{j=1}^{n} a_{ij}\right)^{\frac{1}{n}}}{\sum_{k=1}^{n}\left(\prod_{j=1}^{n} a_{kj}\right)^{\frac{1}{n}}} \tag{8}$$

where i = 1, 2, . . ., n; n is the number of feature quantities.

(c) Eigenvalue method. First, the maximum eigenvalue of matrix $\boldsymbol{A}$ and its corresponding eigenvector are solved. Then, the eigenvector is normalized to obtain the final weight vector.

In order to ensure the scientificity and accuracy of the final weights, we take the average of the weight results calculated by the three methods to obtain the final weights. We use MATLAB to calculate them. The final obtained subjective weight vector is denoted as V = [0.2086, 0.0510, 0.1043, 0.4275, 0.2086]$^{\mathrm{T}}$. The weight allocation results show that channel environmental conditions ($\mathbf{k_4}$) have the highest weight (0.4275), followed by maximum temperature sag/span length ($\mathbf{k_1}$) and historical clearance situations ($\mathbf{k_5}$), each accounting for 0.2086. This quantitative result is consistent with field operation and maintenance experience: channel environment has the greatest impact on the line's heat dissipation capacity and is the primary consideration in assessing weak spans.

3.2. Preprocessing of Raw Feature Data

Aiming at the different characteristics of the raw data, we adopt different preprocessing methods [28]. Maximum temperature arc sag/segment length, channel environmental conditions, and historical clearing times do not have too many outliers present, so the Min–Max normalization method is selected for processing, with the formula shown in Equation (9).

$$y = \frac{x - min}{max - min} \tag{9}$$

Aiming at clearance hazard points and cross-crossing situations, the original data are prone to abnormal values, resulting in a serious deviation in the assessment results of one or more segments. We use stepwise processing. If the original data are less than or equal to 10, the value is assigned directly to 1; if they are greater than 10, the value is assigned to 1.5. The formula is shown in Equation (10).

$$\mathrm{y} = \begin{cases} 0 < x \leq 10\ ,\ 1 \\ x \geq 10\ ,\ 1.5 \end{cases} \tag{10}$$

After the above processing, the numerical values of most of the raw data remains within the range of [0, 1], and only a very small portion of the data in the headroom hazard points and cross-crossing points will have a value of 1.5, which will not have an impact on the overall assessment and will satisfy the requirements of data preprocessing.

3.3. Transmission Line Segments Condition Assessment Classification and Characteristic Indicator Boundaries

With reference to the grid operation and maintenance guidelines, operation and maintenance standards and other documents, the results of the transmission line segment assessment are divided into four grades, which are excellent, good, fair, and poor. They are denoted by the letters G1, G2, G3, and G4, and the monitoring opinions corresponding to each grade are shown in Table 4. The grade boundaries are delineated as shown in Table 5.

Table 4. Evaluation levels and maintenance measures.

Level	Maintenance Measures
Excellent(G1)	The segment status is excellent, enabling maintenance-free operation
Good(G2)	The segment status is good, and should be monitored periodically
Fair(G3)	The characteristic features are showing a degradation trend, and some parameters should be monitored in real-time
Poor(G4)	The characteristic values are significantly exceeding the standard, making it crucial to monitor them in real-time as a vulnerable point

Table 5. Characteristic quantity index level boundaries.

Characteristic Quantity	Excellent	Good	Fair	Poor
Maximum temperature sag/span length $\mathbf{k_1}$/%	2%	3%	4%	5%
Headroom hazardous point $\mathbf{k_2}$/each	0	3	6	10
Cross-crossing $\mathbf{k_3}$/each	0	1	2	3
Channel environment conditions $\mathbf{k_4}$/level	1	2	3	4
Historical clearance situations $\mathbf{k_5}$/each	0	0	1	2

Based on the preprocessing methodology described in the previous subsection, the divided indicator limits were systematically processed, yielding the normalized data results presented in Table 6.

Table 6. The processed boundary data.

Characteristic Quantity	Excellent	Good	Fair	Poor
Maximum temperature sag/span length $\mathbf{k_1}$/%	0.143	0.214	0.286	0.357
Headroom hazardous point $\mathbf{k_2}$/each	0	1	1	1.5
Cross-crossing $\mathbf{k_3}$/each	0	1	1	1
Channel environment conditions $\mathbf{k_4}$/level	0.1	0.2	0.3	0.4
Historical clearance situations $\mathbf{k_5}$/each	0	0	0.5	1

This procedure strictly adheres to the established data standardization protocol, ensuring that all indicator boundary values are comparable under a unified measurement scale, thereby providing a reliable data foundation for subsequent evaluation and analysis.

Using the preprocessed grade limits, by multiplying each grade limit by its corresponding weight, we obtain a weighted value for each grade, calculated as shown in Equation (11).

$$f_j = \sum_{i=1}^{5} \omega_i r_{ji} \tag{11}$$

where ω_i is the feature quantity weight; r_{ji} is the limit value corresponding to the four status levels after preprocessing, with excellent, good, fair, and poor in turn corresponding to j taken as 1, 2, 3, 4.

After calculation we obtain the vector of grade boundaries $\boldsymbol{F}$ = [0.073, 0.285, 0.448, 0.769]^T corresponding to the four grades. These four threshold values quantitatively divide the operating condition into four state levels: a score below 0.073 is classified as "Excellent," 0.073–0.285 as "Good," 0.285–0.448 as "Moderate," and above 0.448 as "Poor." In particular, a score exceeding 0.769 indicates that the span condition deviates substantially from the normal range and should be flagged as a vulnerable point for prioritized monitoring.

3.4. Determination of Assessment Results

First of all, the fuzzy comprehensive evaluation used in the subsequent assessment-grade judgment is introduced. It is an evaluation method based on fuzzy logic theory. It applies fuzzy set theory to the grading indices of the evaluation object. It fuzzifies these indices, determines the fuzzy relationship between the grades, and transforms the fuzzy evaluation results into specific values or grades, so as to make comparisons and analyses.

The fuzzy comprehensive evaluation result is obtained by multiplying the original data of each segment distance with the processed feature weights, and its formula is shown in the following Equation (12).

$$f = \sum_{i=1}^{5} \omega_i p_i \tag{12}$$

where p_i is each component of the original data after processing, and ω_i is the corresponding weight value of the feature quantities.

According to the fuzzy comprehensive evaluation method. $\boldsymbol{F} = (f_1, f_2, f_3, \ldots, f_n)$, if $|f_m - f| = \min\{|f_i - f|\}$ $(i = 1, 2, \ldots, n)$, the level to which the thing being evaluated belongs is the mth level. In this way we can get both qualitative and quantitative assessment results, thus realizing the comprehensive evaluation of transmission line segments.

4. Case Analysis

The 110 kV line of a power grid company has a total of 39 spans and is a double-circuit line on the same tower, with a total length of 2 × 11.9 km. The conductor uses a single LGJ-400/35 steel-core rare-earth aluminum stranded wire (GB/T 1179-2017 [29] technical standard). There are two ground wires: one of them is a 24-core OPGW composite optical cable, and the other uses an LGJ-70/40 steel-core rare-earth aluminum stranded wire. The landform along the line is mainly mountainous, with large relief, and an elevation range of 4.0–350.0 m. Transportation is difficult, and most of the areas have no ready-made roads for access. In the mountains and hills, transportation basically relies on manpower, and the terrain crossed by the line is complex. The topographic classification is shown in Table 7 below. The quantitative statistics in Table 7 show that the mountainous section extends up to 8.0 km, accounting for 67% of the total line length. This indicates that most segments of the line face challenges such as poor heat dissipation conditions and difficult inspection, thereby increasing the likelihood of vulnerable spans. After the steps of preprocessing and fuzzy comprehensive evaluation described in the previous subsection, we obtained the evaluation results for each segment of the line, and the raw data and evaluation results are shown in Table 8.

Table 7. Topographic distribution.

Landform	Mountainous Region	Hill	Flat
Transmission line length/km	8.0	3.2	0.7
Account for the proportion of the whole line/%	67%	27%	6%

According to the results of fuzzy comprehensive evaluation and weighted calculation, the top three ranking results of transmission line segment weakness are spans #34–35, #22–#23, and #28–#29. As indicated by the quantitative data in Table 8, the composite scores of these three spans are 0.6951, 0.6897, and 0.6861, respectively. All of them exceed the "Poor" boundary value of 0.448 and are close to the severe-deviation threshold of 0.769. A closer look at the characteristic quantities shows that: for span #34–#35, the channel environmental condition ($\mathbf{k_4}$ = 3) receives a relatively high score, corresponding to poor heat dissipation; for span #22–#23, the crossing condition ($\mathbf{k_3}$ = 5) is far higher than that of

other spans, and the maximum-temperature sag-to-span-length ratio ($\mathbf{k_1}$ = 4.32%) is also at a relatively high level; for span #28–#29, both the historical clearance count ($\mathbf{k_5}$ = 2) and the clearance-risk points ($\mathbf{k_2}$ = 2) take relatively high values. Taken together, these quantitative indicators consistently point to the vulnerability of the three spans. We then communicated with operation and maintenance personnel to understand the specific condition of each span and to verify the reliability of the results. The specific situation of each span is described below.

Table 8. The raw data and evaluation results.

Segment Number	k_1	k_2	k_3	k_4	k_5	f	Level
#34–#35	3.35%	1	0	3	1	0.6951	Poor
#22–#23	4.32%	0	5	3	0	0.6897	Poor
#28–#29	3.97%	2	0	2	2	0.6861	Poor
#11–#12	4.20%	0	1	3	0	0.6839	Poor
#33–#34	5.40%	0	0	3	0	0.6361	Poor
#21–#22	2.58%	0	2	3	0	0.6078	Fair
#09–#10	3.67%	1	0	2	1	0.5677	Fair
#20–#21	3.65%	1	0	2	1	0.5669	Fair
#31–#32	3.06%	6	0	2	1	0.5391	Fair
#03–#04	4.07%	0	1	2	0	0.5355	Fair
#30–#31	2.86%	5	0	2	1	0.5296	Fair
#18–#19	2.54%	0	0	3	0	0.5015	Fair
#07–#08	4.98%	0	0	2	0	0.4738	Fair
#16–#17	4.86%	0	0	2	0	0.4682	Fair
#29–#30	3.17%	0	0	1	2	0.4549	Fair
#02–#03	3.70%	12	2	1	0	0.4520	Fair
#19–#20	4.28%	0	0	2	0	0.4411	Fair
#38–#39	3.51%	0	0	2	0	0.4046	Fair
#25–#26	3.60%	0	0	1	1	0.3706	Fair
#08–#09	2.75%	0	0	2	0	0.3689	Fair
#15–#16	2.73%	0	0	2	0	0.3679	Fair
#36–#37	2.23%	0	0	2	0	0.3447	Good
#00–#01	4.67%	0	0	1	0	0.3167	Good
#24–#25	3.22%	0	0	1	0	0.2486	Good
#01–#02	3.14%	0	0	1	0	0.2447	Good
#27–#28	3.07%	0	0	1	0	0.2416	Good
#04–#05	4.81%	1	0	0	0	0.2318	Good
#26–#27	2.84%	0	0	1	0	0.2309	Good
#13–#14	2.10%	1	0	0	1	0.2085	Good
#12–#13	2.49%	0	2	0	0	0.1761	Excellent
#23–#24	1.60%	0	0	1	0	0.1724	Excellent
#35–#36	4.47%	0	0	0	0	0.1649	Excellent
#32–#33	2.10%	0	1	0	0	0.1579	Excellent
#06–#07	2.04%	0	0	0	1	0.1550	Excellent
#37–#38	3.12%	1	0	0	0	0.1523	Excellent
#14–#15	3.55%	0	0	0	0	0.1214	Excellent
#17–#18	3.22%	0	0	0	0	0.1059	Excellent
#10–#11	2.47%	0	0	0	0	0.0708	Excellent
#05–#06	0.96%	0	0	0	0	0.0000	Excellent

The real view of span #34–#35 is shown in Figures 6 and 7. The transmission line is located in a valley terrain, which often presents a relatively closed environment that restricts air flow and impedes air circulation. This topographic feature leads to poor heat dissipation, making transmission lines more vulnerable to heat buildup. Second, the valley topography makes the temperature gradient relatively small, and the temperature

difference between different heights is limited, thus limiting the heat dissipation process. At the same time, the valley topography may cause changes in local meteorological conditions, forming temperature inversions and other phenomena, increasing the heat accumulation and temperature inhomogeneity faced by the transmission line, making it a weak link in the system that needs special attention.



Figure 6. Real view of segment #34–#35 1.



Figure 7. Real view of segment #34–#35 2.

The real view of span #22–#23 is shown in Figures 8 and 9. The spacing is longer. First, an excessively long span can cause the transmission line conductor to be subjected to a large horizontal tension. Such a force will create additional tension on the wire, increasing the stress on the wire, which may cause the wire to bend or deform, which in turn affects the conductive properties of the wire. At the same time, a long span can also create additional torque and pressure on line support structures, such as clamps or splices. Long-distance line laying increases the stress points of the support structure, resulting in a greater load on the clamp or connecting pipe, so they must be strong and stable enough to withstand this additional moment and pressure. In addition, the sag of this span is large, and there may be a risk of conductor failure. Moreover, there are many cross-crossing situations in this span, and the facilities under the line are complicated, which increases operational instability.



Figure 8. Real view of segment #22–#23 1.



Figure 9. Real view of segment #22–#23 2.

The real view of span #28–#29 is shown in Figures 10 and 11. The span is located near the foot of the mountain, where convection is relatively weak, and the trees below the line grow faster, creating greater safety risks when the sag increases. First, an increase in the sag means that the wire sags more, reducing the distance between the wire and the tree. This proximity may cause the tree's branches to come into direct contact with the wires, which increases the risk of a short circuit or other electrical failure. This not only poses a threat to the line itself but may also pose a potential danger to the surrounding environment and personnel safety. In addition, fast-growing trees may result in reduced clearance between transmission lines and trees. This can cause the temperature of the line to increase during high load operation, increasing the clearance danger point of the transmission line and causing potential hazards.



Figure 10. Real view of segment #28–#29 1.



Figure 11. Real view of segment #28–#29 2.

Finally, based on the LiPowerline software V5.0, we developed an intelligent computation module for identifying and ranking vulnerable spans. The module provides: (1) a manual input interface for channel environmental conditions and the historical number of fault-clearance events, with support for saving intermediate files; (2) one-click retrieval

of data generated in LiPowerline, including "crossing analysis", "clearance-risk points" and "maximum-temperature sag"; (3) automatic parameter integration and span ranking according to the computed vulnerability level. The module can automatically complete the computation and generate a report. After computation, a ranked list of span vulnerabilities for each grade can be obtained, together with an exported report file.

5. Conclusions

This paper proposes a transmission line segment assessment method based on correlation analysis and the Analytic Hierarchy Process. The former utilizes Pearson correlation analysis to construct a system of evaluation indicators, and the latter effectively addresses the problem of overly subjective weight allocation. Finally, the accuracy and effectiveness of the method are verified through actual cases, which can reflect the status of transmission line segments from both qualitative and quantitative aspects, and the software implementation of the calculation model has also been completed.

In this paper, the environmental conditions of the channel and the number of historical clearances, which have a greater impact on the weakness of the line segments, are added in the construction of the feature quantity system. When building the assessment model, it is graded based on the fuzzy comprehensive evaluation method so as to realize a dual qualitative and quantitative assessment.

The future focus will be on studying the method of obtaining the weights of feature quantities using machine learning. Methods to ensure the accuracy of the assessment results in the absence of feature parameters will also be explored.

Author Contributions: Conceptualization, S.L. and H.M.; methodology, Y.M.; software, W.Y.; validation, X.E.; formal analysis, Y.H.; investigation, Y.H.; resources, H.M.; writing—review and editing, J.L.; funding acquisition, S.L. All authors have read and agreed to the published version of the manuscript.

Funding: This research was funded by the Science and Technology Project of China Southern Power Grid Company Limited (CGYKJXM20240218).

Data Availability Statement: The data presented in this study are available on request from the first author.

Acknowledgments: We sincerely appreciate the valuable comments and suggestions provided by the editors and reviewers to enhance this research.

Conflicts of Interest: Authors Shizeng Liu, Yigang Ma, Wenbin Yu, and Xianzhong E were employed by Dali Bureau, EHV Power Transmission Company of China Southern Power Grid. The remaining authors declare that the research was conducted in the absence of any commercial or financial relationships that could be construed as a potential conflict of interest.

References

1. Mbuli, N.; Xezile, R.; Motsoeneng, L.; Ntuli, M.; Pretorius, J.-H. A literature review on capacity uprate of transmission lines: 2008 to 2018. *Electr. Power Syst. Res.* **2019**, *170*, 215–221. [CrossRef]
2. Xu, J.-H.; Lu, Y.; Bai, G.; Chi, Y.; Su, L. Power investment and transmission network expansion in China and its neighbouring countries towards carbon neutrality. *J. Clean. Prod.* **2023**, *433*, 139626. [CrossRef]
3. Rintamäki, T.; Oliveira, F.; Siddiqui, A.S.; Salo, A. Achieving emission-reduction goals: Multi-period power-system expansion under short-term operational uncertainty. *IEEE Trans. Power Syst.* **2023**, *39*, 119–131. [CrossRef]
4. Li, J.; Lin, J.; Han, Y.; Zhu, L.; Chang, D.; Shao, C. Overload Risk Assessment of Transmission Lines Considering Dynamic Line Rating. *Energies* **2025**, *18*, 1822. [CrossRef]
5. Han, X. Research and Application of Thermal Path Model in Dynamic Capacity Increasing Technology. *Henan Sci. Technol.* **2019**, *29*, 150–152.
6. Yang, B.; Li, W.; Zhao, Y.; He, X. Design and analysis of a grid-connected photovoltaic power system. *IEEE Trans. Power Electron.* **2009**, *25*, 992–1000. [CrossRef]

7. Dupin, R.; Kariniotakis, G.; Michiorri, A. Overhead lines dynamic line rating based on probabilistic day-ahead forecasting and risk assessment. *Int. J. Electr. Power Energy Syst.* **2019**, *110*, 565–578. [CrossRef]
8. Ou, J.; Yuan, J.; Tian, J.; Zhang, W.; Cao, W.; Bai, K. Technical analysis of power transmission line construction in complex environment. In *Proceedings of the 2024 5th International Conference on Artificial Intelligence and Electromechanical Automation (AIEA)*; IEEE: New York, NY, USA, 2024; pp. 539–542.
9. Racz, L.; Szabo, D.; Gocsei, G.; Nemeth, B. Grid Management Technology for The Integration of Renewable Energy Sources into The Transmission System. In *Proceedings of the 2018 7th International Conference on Renewable Energy Research and Applications (ICRERA), Paris, France, 14–17 October 2018*; IEEE: New York, NY, USA, 2018; pp. 612–617.
10. Zhang, C.; Lin, R.; Zhang, N. Cross-Section Optimization Method of Overhead Transmission Lines for Onshore Wind Farms Considering Dynamic Ampacity Increasing. *Electr. Power Eng. Technol.* **2019**, *38*, 86–91.
11. Theodorakatos, N.P.; Babu, R.; Theodoridis, C.A.; Moschoudis, A.P. Mathematical Models for the Single-Channel and Multi-Channel PMU Allocation Problem and Their Solution Algorithms. *Algorithms* **2024**, *17*, 191. [CrossRef]
12. Manousakis, N.M.; Korres, G.N. Optimal PMU arrangement considering limited channel capacity and transformer tap settings. *IET Gener. Transm. Distrib.* **2020**, *14*, 5984–5991. [CrossRef]
13. Theodorakatos, N.P.; Babu, R.; Moschoudis, A.P. The branch-and-bound algorithm in optimizing mathematical programming models to achieve power grid observability. *Axioms* **2023**, *12*, 1040. [CrossRef]
14. Khalyasmaa, A.I.; Uteuliyev, B.A.; Tselebrovskii, Y.V. Methodology for analysing the technical state and residual life of overhead transmission lines. *IEEE Trans. Power Deliv.* **2020**, *36*, 2730–2739. [CrossRef]
15. Yang, C.; Zhong, H.; Huang, X. Construction of Key Index System for Transmission Line Condition Evaluation Based on Confidence Analysis and Improved PCA. *Power Syst. Autom.* **2023**, *45*, 89–94.
16. Wu, Z. Early Warning Methods for Safety Hazards in Transmission Lines. *Autom. Appl.* **2023**, *64*, 133–135+154.
17. Wei, Z.; Gong, H.; Jiang, L.; Liu, J.-Y.; Zhu, G.-J.; Dai, S.-L. Comprehensive risk based operational status assessment of transmission line. In *Proceedings of the 2014 International Conference on Power System Technology, Chengdu, China, 20–22 October 2014*; IEEE: New York, NY, USA, 2014; pp. 232–237.
18. Huang, Q.; Shao, L.; Li, N. Dynamic detection of transmission line outages using hidden Markov models. *IEEE Trans. Power Syst.* **2015**, *31*, 2026–2033. [CrossRef]
19. Gogtay, N.J.; Thatte, U.M. Principles of correlation analysis. *J. Assoc. Physicians India* **2017**, *65*, 78–81.
20. Vaidya, O.S.; Kumar, S. Analytic hierarchy process: An overview of applications. *Eur. J. Oper. Res.* **2006**, *169*, 1–29. [CrossRef]
21. Yu, D.; Kou, G.; Xu, Z.; Shi, S. Analysis of collaboration evolution in AHP research: 1982–2018. *Int. J. Inf. Technol. Decis. Mak.* **2021**, *20*, 7–36. [CrossRef]
22. Liu, Y.; Eckert, C.M.; Earl, C. A review of fuzzy AHP methods for decision-making with subjective judgements. *Expert Syst. Appl.* **2020**, *161*, 113738. [CrossRef]
23. Chen, C.; Yang, B.; Song, S.; Peng, X.; Huang, R. Automatic clearance anomaly detection for transmission line corridors utilizing UAV-borne LiDAR data. *Remote Sens.* **2018**, *10*, 613. [CrossRef]
24. Karimi, S.; Musilek, P.; Knight, A.M. Dynamic thermal rating of transmission lines: A review. *Renew. Sustain. Energy Rev.* **2018**, *91*, 600–612. [CrossRef]
25. De Winter, J.C.; Gosling, S.D.; Potter, J. Comparing the Pearson and Spearman correlation coefficients across distributions and sample sizes: A tutorial using simulations and empirical data. *Psychol. Methods* **2016**, *21*, 273. [CrossRef]
26. Benesty, J.; Chen, J.; Huang, Y.; Cohen, I. Pearson correlation coefficient. In *Noise Reduction in Speech Processing*; Springer: Berlin/Heidelberg, Germany, 2009; pp. 1–4.
27. Myers, L.; Sirois, M.J. Spearman correlation coefficients, differences between. *Encycl. Stat. Sci.* **2004**, *12*, 7901–7903.
28. McCarthy, D.J.; Campbell, K.R.; Lun, A.T.; Wills, Q.F. Scater: Pre-processing, quality control, normalization and visualization of single-cell RNA-seq data in R. *Bioinformatics* **2017**, *33*, 1179–1186. [CrossRef]
29. *GB/T 1179-2017*; Round Wire Concentric Lay Overhead Electrical Stranded Conductors. General Administration of Quality Supervision, Inspection and Quarantine of the People's Republic of China. Standardization Administration of the People's Republic of China: Beijing, China, 2017.

Disclaimer/Publisher's Note: The statements, opinions and data contained in all publications are solely those of the individual author(s) and contributor(s) and not of MDPI and/or the editor(s). MDPI and/or the editor(s) disclaim responsibility for any injury to people or property resulting from any ideas, methods, instructions or products referred to in the content.